Optical properties of low band gap alternating copolyfluorenes for photovoltaic devices

ARTICLE *in* THE JOURNAL OF CHEMICAL PHYSICS · DECEMBER 2005

Impact Factor: 2.95 · DOI: 10.1063/1.2087367 · Source: PubMed

5 AUTHORS, INCLUDING:

Mengtao Sun
Chinese Academy of Sciences
129 PUBLICATIONS **2,722** CITATIONS
SEE PROFILE

Tönu Pullerits
Lund University
178 PUBLICATIONS **5,379** CITATIONS
SEE PROFILE

Excited State Properties of the Chromophore of the asFP595 Chromoprotein: 2D and 3D Theoretical Analyses

MENGTAO SUN

Department of Chemical Physics, Lund University, Lund SE221 00, Sweden

Received 5 July 2005; accepted 11 July 2005
Published online 3 October 2005 in Wiley InterScience (www.interscience.wiley.com).
DOI 10.1002/qua.20815

ABSTRACT: The ground and excited state properties (e.g., the intramolecular charge and energy transfer, and electron-hole coherence) of the chromophore of the asFP595 chromoprotein from *Anemonia sulcata* in the neutral and anionic forms are theoretically studied with quantum chemistry methods. The ground-state properties of the asFP595 in the neutral and anionic forms, such as the alternations of the bond lengths and the Mulliken charge distributions, are compared. The calculated transition energies of the asFP595 in the neutral and anionic form are consistent with the experimental results. To study the excited state properties of the asFP595 chromophore, the energies and densities of highest occupied molecular orbitals (HOMOs) and lowest unoccupied molecular orbitals (LUMOs), as well as the CI main coefficients, are compared between the two forms. The intramolecular charge and energy transfer in the neutral and anionic forms are investigated and compared with the three-dimensional (3D) real-space analysis methods, including the strength and orientation of the transition dipoles with transition density, and the orientation and result of the intramolecular charge transfer with charge difference density. The electron-hole coherence and delocalization on the excitation are studied with the 2D real-space analysis method of the transition density matrix. In all, the calculated results are remain in good agreement with the experimental data, and the theoretical analysis results supported the proposed models in the experiment. Int J Quantum Chem 106: 1020–1026, 2006

Key words: asFP595 chromoprotein; intramolecular charge and energy transfer; electron-hole coherence

Contract grant sponsor: NNSFC.
Contract grant number: 10374040.
Contract grant sponsor: Wenner–Gren Foundation of Sweden.

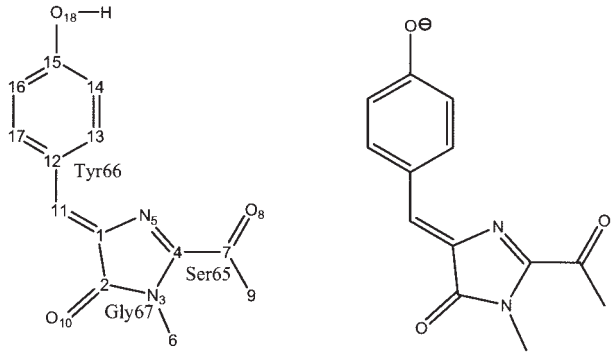

FIGURE 1. asFP595 chromophore in the neutral and anionic forms.

Introduction

Since the green fluorescence protein (GFP) was discovered as a companion protein to aequorin, the chemiluminescent protein from *A. Victoria* [1], it was extensively used in molecular and cell biology as a noninvasive genetically encoded fluorescent label [2]. Its unique ability to synthesize chromophore within itself, without any need for external substrates or cofactors except molecular oxygen [3], made it an excellent in vivo marker of gene expression and protein localization in various biological systems [4]. The GFP chromophore is composed of two rings, Tyr66, Gly67 and a side chain Ser65 [5] (see in Fig. 1), and is formed from the autocatalytic process consisting of two main steps: cyclization of the protein backbone at positions 65–67 (Ser-Tyr-Gly), followed by dehydrogenation of the Tyr66 side chain [6–9]. This structure is a system of conjugated double bonds capable of absorbing and emitting light in the visible region [5]; and the intramolecular charge and energy can occur on the photoinduced dynamics. It is important to study the intramolecular charge and energy transfer [10, 11] and electron coherence [12, 13] on photoinduced dynamics processes. There are two forms for the asFP595 chromophore in the Ph-dependent solvents [5, 14]: one is the neutral form at acidic pH, and the other is the anionic form at neutral and slightly basic pH [5].

To study the excited properties of the conjugated molecules in the excited state, including the charge and energy transfer, and electron-hole coherence, several elaborate theoretical approaches have been used to visually inspect all molecular orbitals contributing to the excitation for large conjugated carotenoids and polymers. One is the two-dimensional (2D) real-space analysis of transition density matrix, representing the electronic transition between the ground state and the electronically excited state [12–17], which is used to analyze the electron-hole coherence and the excitation delocalization of conjugated molecules. The other is the 3D real-space analysis of transition density (TD) and charge difference density (CDD) [18–21], which has been used to analyze the charge and energy transfer in several conjugated polymers. The combination of the 2D and 3D real-space analysis methods has been employed to study the excited state properties of conjugated polymers [22, 23].

In this study, the ground-state and excited state properties of the asFP595 chromophore in the neutral and the anionic form are investigated with quantum chemistry methods. From the optimized ground-state geometries, the alternation of the bond lengths and Mulliken charge distribution are compared between the neutral and anionic forms. The calculated transition energies are compared with the experimental data. To study the excited state properties of the asFP595 chromophore, the energies and densities of highest occupied molecular orbitals (HOMOs) and lowest unoccupied molecular orbitals (LUMOs), as well as the CI main coefficients, are compared between the two forms. Furthermore, the intramolecular charge and energy transfer are studied with the 3D real-space analysis method: (i) the orientation and strength are studied with the transition densities, which determine the dipole transition moment (or transition dipole) [22]; and (ii) the orientation and results of the charge transfer are also studied with charge difference densities [23]. Lastly, the electron-hole coherences of the asFP595 chromophore on the photoinduced dynamics are studies with the 2D real-space analysis method of transition density matrix.

Methods

The geometry optimizations of the asFP595 chromophore are performed for the ground state with density functional theory (DFT) [24] with B3LYP function [25] and basis set 6-31G+(D) [26]. The electronic excited states of the asFP595 chromophore have been computed, using the time-dependent density functional theory (TD-DFT) method [27] with the same functional and the basis set, and with key words [22] pop=full and iop(9/40 = 2), as implemented in Gaussian 03 [28]. The

electronic excited states of the asFP595 chromophore have also been computed, using the TD-DFT method [27] with the B3LYP functional and the SV (*P*) basis set, as implemented in Turbomole [29].

As results from the TD-DFT calculation, the singlet excited states $|S_n\rangle$ are represented by vectors $C^{CI}_{n,ai}$ based on configurations of unoccupied and occupied molecular orbitals *a* and *i*, respectively. The molecular orbitals are, in turn, given by linear combinations of atomic orbitals (LCAO) μ and ν with coefficients $c^{LCAO}_{a\mu}$ and $c^{LCAO}_{i\nu}$. To characterize the excited state by observables, we define two matrices [30]:

$$Q^{(n)}_{\mu\nu} = \frac{1}{\sqrt{2}} \sum_{\substack{a\in unocc \\ i\in occ}} C^{CI}_{n,ai}(c^{LCAO}_{a\mu}c^{LCAO}_{i\nu} + c^{LCAO}_{i\mu}c^{LCAO}_{a\nu})$$

$$P^{(n)}_{\mu\nu} = \frac{i}{\sqrt{2}} \sum_{\substack{a\in unocc \\ i\in occ}} C^{CI}_{n,ai}(c^{LCAO}_{a\mu}c^{LCAO}_{i\nu} - c^{LCAO}_{i\mu}c^{LCAO}_{a\nu}), \quad (1)$$

which are (anti)symmetric for exchange of the atomic orbitals and normalized as

$$\sum_{\mu,\nu} |Q^{(n)}_{\mu\nu}|^2 = \sum_{\mu,\nu} |P^{(n)}_{\mu\nu}|^2 = 1. \quad (2)$$

In the collective electron oscillator (CEO) model [12], the excited state $|S_n\rangle$ is described by a harmonic oscillator with oscillating coordinate $Q^{(n)}_{\mu\nu}\cos(\omega_n t)$ and momentum $P^{(n)}\sin(\omega_n t)$ for the transition frequency ω_n. For visual characterization of the excited states, we use two different representations of the matrices $Q^{(n)}_{\mu\nu}$ and $P^{(n)}_{\mu\nu}$.

REAL-SPACE REPRESENTATION

In real space, the oscillating CEO coordinate and momentum are given as [30]

$$Q_n(\mathbf{r}, \mathbf{r}'; t) = \sum_{\mu\nu} \phi^{AO}_\mu(\mathbf{r}) Q^{(n)}_{\mu\nu} \phi^{AO}_\nu(\mathbf{r}')\cos(\omega_n t)$$

$$P_n(\mathbf{r}, \mathbf{r}'; t) = \sum_{\mu\nu} \phi^{AO}_\mu(\mathbf{r}) P^{(n)}_{\mu\nu} \phi^{AO}_\nu(\mathbf{r}')\sin(\omega_n t). \quad (3)$$

The diagonal slice for $\mathbf{r} = \mathbf{r}'$ results in

$$Q_n(\mathbf{r}, \mathbf{r}; t) = \sqrt{2}\,\rho_{n0}(\mathbf{r})\cos(\omega t)$$

$$P_n(\mathbf{r},\mathbf{r};t) = 0. \quad (4)$$

The amplitude of the former is given by the so-called transition density (TD)

$$\rho_{n0}(\mathbf{r}) = \frac{1}{\sqrt{2}} \sum_{\mu,\nu} \phi^{AO}_\mu(\mathbf{r}) Q^{(n)}_{\mu\nu} \phi^{AO}_\nu(\mathbf{r}). \quad (5)$$

The transition density contains information about the spatial location of the excitation [21] and is directly related to the transition dipole

$$\boldsymbol{\mu}_{n0} = e \int \mathbf{r}\rho_{n0}(\mathbf{r}) d^3r. \quad (6)$$

Furthermore, it is of particular relevance for excitonic interaction at shorter distance [20].

Besides the transition density, the charge difference density (CDD) [19]

$$\Delta\rho_{nn}(\mathbf{r}) = 2i \sum_{\mu,\nu,\kappa} \phi^{AO}_\mu(\mathbf{r}) Q^{(n)}_{\kappa\mu} P^{(n)}_{\kappa\nu} \phi^{AO}_\nu(\mathbf{r}) \quad (7)$$

is another useful quantity for real-space characterization of excitons. It represents the difference in electron distribution between the excited state $|S_n\rangle$ and the ground state $|S_0\rangle$. In the present work, both transition and charge difference density are represented by isosurfaces based on a 3D grid of ~100,000 cubes.

SITE REPRESENTATION

For site representation of the CEO coordinate and momentum, we define

$$\overline{Q^{(n)2}_{AB}} = \sum_{\substack{\mu\in A \\ \nu\in B}} |Q^{(n)}_{\mu\nu}|^2 \quad \text{and} \quad \overline{P^{(n)2}_{AB}} = \sum_{\substack{\mu\in A \\ \nu\in B}} |P^{(n)}_{\mu\nu}|^2, \quad (8)$$

respectively [12, 17]. This means that the matrices $Q^{(n)}_{\mu\nu}$ and $P^{(n)}_{\mu\nu}$ are merged for atomic orbitals μ and ν belonging to atomic sites A and B, respectively. Thus $\overline{P^{(n)2}_{AB}}$ gives the atomic sites A and B where electron and hole oscillate from and to, while $\overline{Q^{(n)2}_{AB}}$ is a measure of the delocalization of the exciton as a whole. Note that for Frenkel excitons, the occupation of $\overline{Q^{(n)2}_{AB}}$ and $\overline{P^{(n)2}_{AB}}$ is limited to pairs of atomic centers A and B belonging to the same monomeric unit.

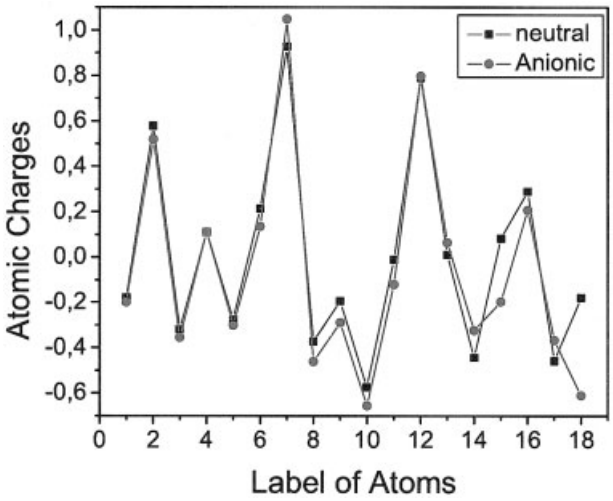

FIGURE 2. Comparison of atomic charges of asFP595 chromophore (atomic charges with hydrogens summed into heavy atoms) between neutral and the anionic forms. Horizontal axis labels represent individual atoms in numbering sequence shown in Fig. 1.

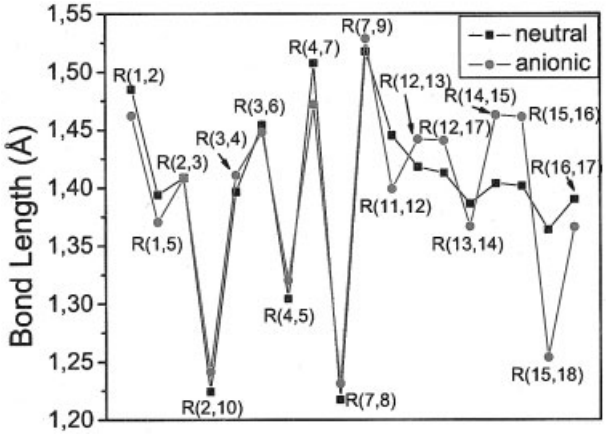

FIGURE 3. Comparison of bond length of asFP595 chromophore between neutral and anionic forms.

Results and Discussion

The optimized ground-state geometries of the asFP595 chromophore in the neutral and anomic forms are compared. The two rings of Tyr66, Gly67 in the neutral and anomic forms are all coplanar. The atomic charge distributions of the asFP595 chromophore in the neutral and anomic forms are compared (see Fig. 2) from the Mulliken charges, where atomic charges with hydrogens are summed into heavy atoms. One can find that the greatest difference of atomic charges is at oxygen atom 18, because of the changing of the hydrogen bonded to oxygen atom 18 in the neutral and the anionic forms. The alternations of the bond lengths for these two forms are compared, as can be seen in Figure 3. The results show that the single bond lengths are decreased and the double bond lengths are increased. The alternations of the bond lengths due to the uneven distribution of the π electrons over the bonds (Peierls distortion) [31, 32] is also an important feature of the geometry of a conjugated oligomer.

The calculated transition energies and oscillator strengths of the asFP595 chromophore in the neutral and anomic forms are listed in Table I. The calculated results are consistent with the experimental data. To study the excited state properties of the asFP595 chromophore (e.g., the red-shifted absorption spectra in the anionic form, the orientation of charge and energy transfer), the energies and densities of HOMOs and LUMOs as well as the CI main coefficients are compared between the two forms, as can be seen in Figure 4. The orbital transition of the first excited state in the neutral form is mainly from HOMO to LUMO, and the energy separation of the HOMO and LUMO is 3.156 eV, which is slightly larger than the transition energy at 3.002 eV. The relationship between the transition energy and the energy gap of HOMO and HOMO was studied in detail by Tretiak et al. [33]. From the density distribution of the HOMO and the LUMO [34], the charge and energy transfer should from the Tyr66 unit to Gly67 and Ser65 units. The energies of HOMO and LUMO of the asFP595 chromophore in the anionic form are much higher than that of the neutral form. In the case of the anionic form, the orbital transition is mainly from the HOMO to LUMO of the molecular orbital, and the energy separation of the HOMO and LUMO is 2.4762 eV, which is slightly smaller than the transition energy

TABLE I

Calculated transition energies and corresponding oscillator strengths (in parentheses).

	Transition energy (nm)		
Neutral	418[a]	413.01 (0.5522)[b]	406.83 (0.5459)[c]
Anionic	520[a]	480.16 (0.7888)[b]	484.68 (0.67467)[c]

[a] Experimental data from Ref. [5].
[b] Calculated results of Gaussian 03.
[c] Calculated result of the Turbomole.

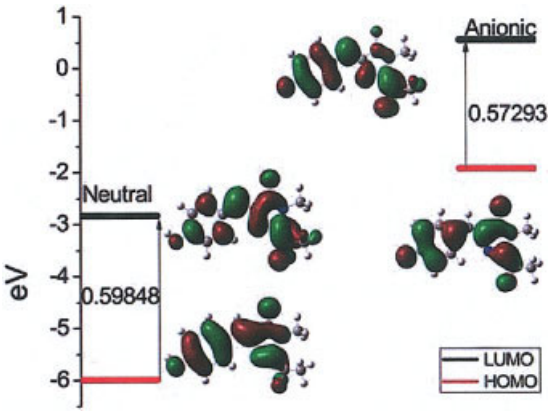

FIGURE 4. Calculated energies and densities of HOMO and LUMO, and CI main coefficients of the orbital transition from HOMO to HUMO. Green and red correspond to different phases of molecular wave functions for HOMO and LUMO; isovalue = 0.02 a.u.

2.583 eV. Because of the decrease in the energy gap of the HOMO and LUMO in the anionic form, the transition energy also is red-shifted.

The excited state properties of the asFP595 chromophore are further studied with the 3D real-space analysis method. Because of the relationship of the transition density and the transition dipole from Eq. (6), the strength and orientation of the transition dipole can be analyzed. From the transition density in the neutral form (see Table II), there are two subunit transition dipoles, one in the Tyr66 ring, and the second one in the Gly67 ring and the Ser65 side chain, there are different orientations for these two subunits, and the orientation is from the holes to the electrons. The relationship of the total transition dipole and the subunit transition dipole for the carotenoid was studied by Tretiak et al. [11]. From the transition density in the anionic form, there is one transition dipole, and the orientation is from the Gly67 ring to the Tyr66 ring. So the transition dipole of the asFP595 chromophore in the anionic form is larger than the total transition dipole of the asFP595 chromophore in the neutral form, which also can be supported by $|\mu_{A,N}|^2 \propto f_{\Omega_{A,N}}/E_{A,N}$ [35], where the oscillator strength of the asFP595 chromophore in the anionic form f_{Ω_A} is larger than that in the neutral form f_{Ω_N}, while the transition energy E_A of the asFP595 chromophore in the anionic form is smaller than that E_N in the neutral form. From the charge difference density in the neutral and anionic forms (see Table II), the charge transfer from the Tyr66 unit to the Ser65 side chain. As a result of the charge transfer, the holes are localized mainly on the two rings, and the charges are localized mainly on the side chain and the bonds that connect the two rings. The charges in the Tyr66 ring in the anionic form are slightly larger than those in the Tyr66 ring in the neutral form, due to the positively charged hydrogen lost in the anionic form.

The CDD can only show the result of the charge transfer, but cannot show us where the holes/electrons from and to. So, the excited state properties of the asFP595 chromophore are further studied with the 2D real-space analysis method. From the contour plot of the transition density matrix, the electron-hole coherences can be studied. The electron hole can show the hole and electron transfer from and to, which is an important supplement to the 3D representation of the charge difference densities of 3D. First, let us study $\overline{Q_{AB}^{(n)2}}$ and $\overline{P_{AB}^{(n)2}}$, which measure the delocalization of the exciton as a whole, and electron and hole oscillate from and to, respectively. For the asFP595 chromophore in the neural form [see Fig. 5(a) and (b)], the electron-hole coherences among atoms 1, 4, 7, 10–12, and 16–17 are strong on the vertical absorption process, which can show the coherence degree among the atoms on the charge and energy transfer, and can also tell us where the holes/electrons are from, and where they go (e.g., the charges on atom 7 are mainly from atoms 1, 4, and 12). In the anionic form, there are similar results for the electron-hole coherence to the

TABLE II

Transition and charge difference densities of the asFP595 chromophore in the neural and anionic forms.*

	Neutral	Anionic
TD (S_1)	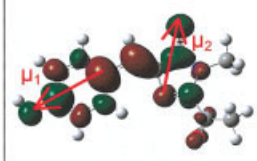	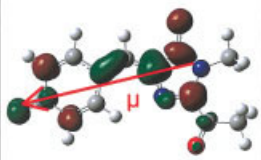
CDD (S_1)	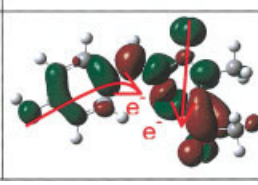	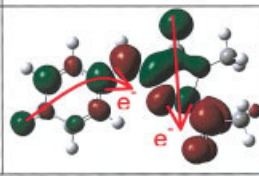

* Green and red represent the hole and electron, respectively. Isovalues are 1×10^{-5} and 4×10^{-4} in atom atoms for TD and CDD, respectively.

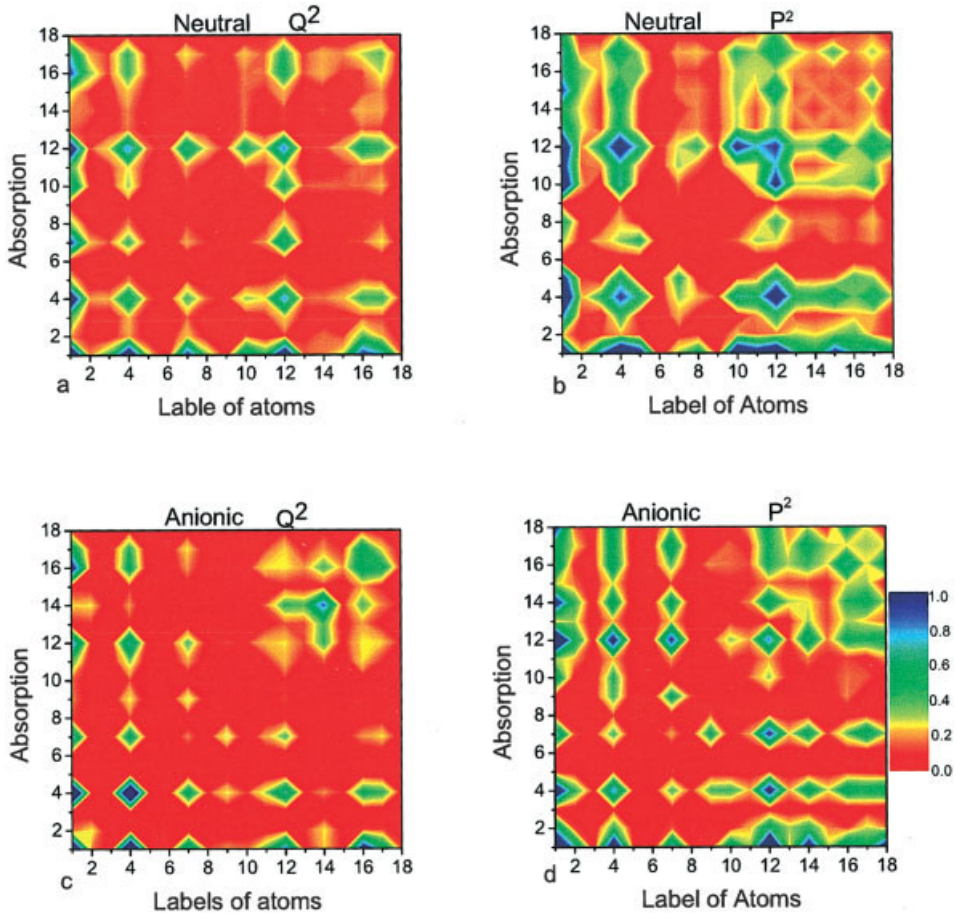

FIGURE 5. Contour plots of transition density matrices. Axis labels represent individual atoms in numbering sequence shown in Fig. 1. Color code is shown on right of (d) (absolute values of matrix elements, scaled to a maximum value of 1.0).

neutral form, but the electron-hole coherence between atoms 12 and 13 (16 and 17) are obviously stronger than those between 12 and 13 (atoms 16 and 17) in the neutral form; and the charges on the atom 7 are mainly from atoms 1, 4, 12, 14, 16). So, comparing the electron-hole coherence from FIgure 5(b) in the neutral form and from Fig. 5(d) in the anionic form, one finds that the electrons and holes oscillate in the Gly67 ring in the anionic form are much stronger than those in the Gly67 ring in the neutral form.

Conclusion

The ground and excited properties of the asFP595 chromophore in the neutral and anionic forms are studied and compared by quantum chemistry methods. The alternations of bond lengths and the atomic charge distribution from the Mulliken charges at the ground excited states are investigated from the optimized ground-state geometries. The excited state properties, such as charge and energy transfer and electron-hole coherence, are studied with the 3D and 2D real-space analysis method.

References

1. Tsien, R. Y. Annu Rev Biochem 1998, 67, 509.
2. Lippincott-Schwartz, J.; Patterson, G. H. Science 2003, 300, 87.
3. Heim, R.; Prasher, D. C.; Tsien, R. Y. Proc Natl Acad Sci USA 1994, 91, 12501.
4. Labas, Y. A.; Gurskaya, N. G.; Yanushevich, Y. G.; Fradkov,

A. F.; Lukyanov, K. A.; Lukyanov, S. A.; Matz, M. V. Proc Natl Acad Sci USA 2002, 99, 4256.
5. Yampolsky, I. V.; James Remington, S.; Martynov, V. I.; Potapov, V. K.; Lukyanov, S.; Lukyanov, K. A. Biochemistry 2005, 44, 5788.
6. Shimomura, O. FEBS Lett 1979, 104, 220.
7. Cody, C. W.; Prasher, D. C.; Wastler, W. M.; Prendergast, F. G.; Ward, W. W. Biochemistry 1993, 32, 1212.
8. Ormo, M.; Cubitt, A. B.; Kallio, K.; Gross, L. A.; Tsien, R. Y.; Remington, S. J. Science 1996, 273, 1392.
9. Yang, F.; Moss, L. G.; Phillips, G. N., Jr. Nat Biotechnol 1996, 4, 1246.
10. Bredas, J. L.; Beljonne, D.; Coropceanu, V.; Cornil, J. Chem Rev 2004, 104, 4971.
11. Tretiak, S.; Chernyak, V.; Mukamel, S. J Am Chem Soc 1997, 119, 11408.
12. Mukamel, S.; Tretiak, S.; Wagersreiter, T.; Chernyak, V. Science 1997, 277, 781.
13. Tretiak, S.; Mukamel, S. Chem Rev 2002, 102, 3171.
14. Niwa, H.; Inouye, S.; Hirano, T.; Matsuno, T.; Kojima, S.; Kubota, M.; Ohashi, M.; Tsuji, F. I. Proc Natl Acad Sci USA 1996, 93, 13617.
15. Tretiak, S.; Saxena, A.; Martin, R. L.; Bishop, A. R. Phys Rev Lett 2002, 89, 097402.
16. Tretiak, S.; Saxena, A.; Martin, R. L.; Bishop, A. R. Proc Natl Acad Sci USA 2003, 100, 2185.
17. Zojer, E.; Buchacher, P.; Wudl, F.; Cornil, J.; Calbert, J. P.; Bredas, J. L.; Leising, G. J Chem Phys 2000, 113, 10002.
18. Krueger, B. P.; Scholes, G. D.; Fleming, G. R. J Phys Chem B 1998, 102, 5378.
19. Beenken, W. J. D.; Pullerits, T. J Phys Chem B 2004, 108, 6164.
20. Beenken, W. J. D.; Pullerits, T. J Chem Phys 2004, 120, 2490.
21. Jespersen, K. G.; Beenken, W. J. D.; Zausjitsyn, Y.; Yartsev, A.; Andersson, M.; Pullerits, T.; Sundström, V. J Chem Phys 2004, 121, 12613.
22. Sun, M. T.; Kjellberg, P.; Ma, F. C.; Pullerits, T. Chem Phys Lett 2005, 401, 558.
23. Sun, M. T. Chem Phys Lett 2005, 408, 128.
24. Dreizler, M. R.; Gross, E. K. U. Density Functional Theory; Springer-Verlag: Heidelberg, 1990.
25. Becke, A. D. J Chem Phys 1993, 98, 5648.
26. Petersson, G. A.; Al-Laham, M. A. J Chem Phys 1991, 94, 6081.
27. Casida, M. E.; Jamorski, C.; Casida, K. C.; Salahub, D. R. J Chem Phys 1998, 108, 4439.
28. Frisch, M. J.; Trucks, G. W.; Schlegel, H. B.; Scuseria, G. E.; Robb, M. A.; Cheeseman, J. R.; Montgomery, J. A.; Vreven, Jr., T.; Kudin, K. N.; Burant, J. C.; Millam, J. M.; Iyengar, S. S.; Tomasi, J.; Barone, V.; Mennucci, B.; Cossi, M.; Scalmani, G.; Rega, N.; Petersson, G. A.; Nakatsuji, H.; Hada, M.; Ehara, M.; Toyota, K.; Fukuda, R.; Hasegawa, J.; Ishida, M.; Nakajima, T.; Honda, Y.; Kitao, O.; Nakai, H.; Klene, M.; Li, X.; Knox, J. E.; Hratchian, H. P.; Cross, J. B.; Adamo, C.; Jaramillo, J.; Gomperts, R.; Stratmann, R. E.; Yazyev, O.; Austin, A. J.; Cammi, R.; Pomelli, C.; Ochterski, J. W.; Ayala, P. Y.; Morokuma, K.; Voth, G. A.; Salvador, P.; Dannenberg, J. J.; Zakrzewski, V. G.; Dapprich, S.; Daniels, A. D.; Strain, M. C.; Farkas, O.; Malick, D. K.; Rabuck, A. D.; Raghavachari, K.; Foresman, J. B.; Ortiz, J. V.; Cui, Q.; Baboul, A. G.; Clifford, S.; Cioslowski, J.; Stefanov, B. B.; Liu, G.; Liashenko, A.; Piskorz, P.; Komaromi, I.; Martin, R. L.; Fox, D. J.; Ketih, T.; Al-Laham, M. A.; Peng, C. Y.; Nanayakkara, A.; Challacombe, M.; Gill, P. M. W.; Johnson, B.; Chen, W.; Wong, M. W.; Gonzalez, C.; Pople, J. A. Gaussian 03; Revision B.05; Gaussian: Pittsburgh, PA, 2003.
29. Ahlrichs, R.; Bär, M.; Baron, H-P.; Bauernschmitt, R.; Böcker, S.; Deglmann, P.; Ehrig, M.; Eichkorn, K.; Elliott, S.; Furche, F.; Haase, F.; Häser, M.; Horn, H.; Hättig, C.; Huber, C.; Huniar, U.; Kattannek, M.; Köhn, A.; Kölmel, C.; Kollwitz, M.; May, K.; Ochsenfeld, C.; Öhm, H.; Patzelt, H.; Rubner, O.; Schäfer, A.; Schneider, U.; Sierka, M.; Treutler, O.; Unterreiner, B.; von Arnim, M.; Weigend, F.; Weis, P.; Weiss, H. Turblemore 5.71; Quantum Chemistry Group; University of Karlsruhe: Karlsruhe, Germany, 2005.
30. Sun, M. T.; Kjellberg, P.; Beenken, W. J. D.; Pullerits, T. J Chem Theory Comput (revision).
31. Bredas, J. L.; Cornil, J.; Beljonne, D.; dos Santos, D.; Shuai, Z. G. Acc Chem Res 1999, 32, 267.
32. Marder, S. R.; Gorman, C. B.; Meyers, F.; Perry, J. W.; Bourhill, G.; Bredas, J. L.; Pierce, B. M. Science 1994, 265, 632.
33. Tretiak, S.; Igumenshchev, K.; Chernyak, V. Phys Rev B 2005, 71, 033201.
34. Cornil, J.; Gueli, I.; Dkhissi, A.; Sancho-Garcia, J. C.; Hennebicq, E.; Calbert, J. P.; Lemaur, V.; Belijonne, D.; Bredas, J. L. J Chem Phys 2003, 118, 6615.
35. Sun, M. T. Chem Phys (in press).